



# Reactivity features of original sol-gel-derived 52S4 glass versus heat treatment temperature

Fatima-Zohra Mezahi<sup>1,2</sup> · Anita Lucas- Girot<sup>3</sup> · Hassane Oudadesse<sup>3</sup> · Abdelhamid Harabi<sup>2</sup>

Received: 27 November 2017 / Revised: 28 March 2018 / Accepted: 10 April 2018 / Published online: 25 April 2018  
© Australian Ceramic Society 2018

## Abstract

This work is devoted to study the reactivity of the quaternary glass 52S4 (52% SiO<sub>2</sub>–30% CaO–14% Na<sub>2</sub>O–4% P<sub>2</sub>O<sub>5</sub> (wt%)), synthesized by sol-gel process versus the treatment temperature. The dried gel was heat treated at 600 and 650 °C and soaked in simulated body fluid (SBF). XRD results confirm the amorphous character of glass treated at 600 °C even though the heat treatment at 650 °C induces Na<sub>2</sub>Ca<sub>2</sub>Si<sub>3</sub>O<sub>9</sub> formation. After soaking in SBF, SEM and EDS results show the formation of carbonated hydroxyapatite (CHA) at the glass surface for both temperatures. For the glasses treated at 600 and 650 °C, two phenomena were observed: the glass dissolution in SBF and the CHA precipitation, but the reactivity kinetics of glass was different when temperature changes. For SGD600, the CHA began to crystallize after 16 h. For SGD650, a glass ceramic made of a glassy matrix and of Na<sub>2</sub>Ca<sub>2</sub>Si<sub>3</sub>O<sub>9</sub>, the crystallized carbonated HA was observed after 2 h. In addition, a new crystallization at the glass surface of Na<sub>2</sub>Ca<sub>2</sub>Si<sub>3</sub>O<sub>9</sub> was observed after 15 days.

**Keywords** Sol-gel process · Temperature · Simulated body fluid · Kinetics reactivity · Bone-like apatite

## Introduction

Bone defect filling or reconstruction required a wide research and development of biocompatible and bioactive materials. The bioactive material, in contact with physiological solutions, elicits a specific biological response at the interface of the material which results in the formation of a direct biochemical link (carbonated hydroxyapatite) when it is implanted in human body [1]. Since Hench has launched the concept of bioactive glass, many new materials and products have been prepared from variations on bioactive glasses [2], glass ceramics [3], and ceramics such as synthetic and natural hydroxyapatite (HA) [4–13], wollastonite [14–16], and diopside [17, 18]. Hench et al. have demonstrated that glass with the molar composition of 46.1% SiO<sub>2</sub>, 24.4 Na<sub>2</sub>O, 26.9 CaO,

and 2.6% P<sub>2</sub>O<sub>5</sub>, termed Bioglass® 45S5, is able to develop, at the interface with body fluids, an apatite-like layer similar to bone mineral. This bond is so strong that it could not be removed without breaking the bone [1]. However, the poor mechanical strength and toughness of bioactive glass have restricted their use in several clinical applications. To resolve this problem, and consequently, to broad the range of clinical applications, the glasses were transformed into glass ceramics [19–21]. Despite these benefits, contradictory results were published on the reactivity and biological interest of these glass ceramics (crystalline or semi-crystalline). They may be less soluble in body fluid and the mineral formation rate and bone integration at the tissue-material interface may be affected [22–24]. At the same time, the crystallization of some glassy systems significantly decreases their bioactivity in comparison with the same amorphous glassy systems [19–21]. Li et al. [25] showed that a bioactive glass can be transformed into an inert glass ceramic. In vitro test showed that the carbonated HA layer was formed only if the glass ceramic contains over 90% of a residual glassy phase. Whereas, Peitl et al. [23, 24] have developed the first bioactive glass ceramic in the SiO<sub>2</sub>–CaO–Na<sub>2</sub>O–P<sub>2</sub>O<sub>5</sub> system with both good mechanical properties and high bioactivity. It contains about 30 to 65% crystalline phase, and the main phase is Na<sub>2</sub>Ca<sub>2</sub>Si<sub>3</sub>O<sub>9</sub>. After that, Ravagnani et al. developed a highly

✉ Fatima-Zohra Mezahi  
mezahif@yahoo.fr

<sup>1</sup> Physics Department, Med Boudiaf University, M'Sila, Algeria

<sup>2</sup> Ceramics Lab. Physics Department, Constantine Mentouri University, Constantine, Algeria

<sup>3</sup> Université de Rennes, CNRS ISCR- UMR6226, 35000 Rennes, France

bioactive fully crystalline glass ceramic in  $\text{SiO}_2\text{--CaO--Na}_2\text{O--P}_2\text{O}_5$  system (Biosilicate® glass ceramic) [26]. Almost all the works have shown that  $\text{Na}_2\text{Ca}_2\text{Si}_3\text{O}_9$  formation, observed in some glass ceramics, enhances the mechanical properties of the starting glass and maintains the high bioactivity of particular compositions in the  $\text{SiO}_2\text{--CaO--Na}_2\text{O--P}_2\text{O}_5$  system. Peitl et al. have shown that glass crystallization decreased development kinetics of a carbonated HA layer but did not inhibit its formation, even in fully crystallized ceramics [24]. In 2011, Siqueira et al. have shown that  $\text{Na}_2\text{Ca}_2\text{Si}_3\text{O}_9$ , formed in  $\text{SiO}_2\text{--CaO--Na}_2\text{O--P}_2\text{O}_5$  system, has bioactivity behavior similar to that of Biosilicate® glass ceramic [27].

In our previous works, a glass with the new composition (wt%) 52%  $\text{SiO}_2$ –30%  $\text{CaO}$ –14%  $\text{Na}_2\text{O}$ –4%  $\text{P}_2\text{O}_5$  (mol%, 52.3%  $\text{SiO}_2$ –32.3%  $\text{CaO}$ –13.7%  $\text{Na}_2\text{O}$ –1.7%  $\text{P}_2\text{O}_5$ ) (named 52S4) was synthesized both by melting and an original sol-gel route [28]. The effect of synthesis mode on glass bioactivity after soaking in simulated body fluid (SBF) was investigated [29]. The dried gel was then heat treated at 550 °C (below the crystallization temperature). The obtained results showed that the main differences between the sol-gel-derived glass (SGDG) and melting-derived glass (MDG), from the structural and textural point of view, are induced by the synthesis mode. The obtained results have led to conclude that 52S4 is a bioactive glass if it is prepared by the two routes: melt and sol-gel. However, this glass was more reactive when it was prepared by sol-gel method. The sol-gel route enhanced fast and continuous glass resorption associated to the early formation of the bone-like apatite at the glass surface. However, the HA did not crystallize even after 30 days. This result was attributed to a continuous formation of silica gel up to the amorphous apatite layer.

The aim of the present study is to investigate a possible evolution in reactivity behavior of the sol-gel-derived glass by increasing the thermal treatment temperature previously used [28, 29].

## Experimental section

### Material preparation

The sol-gel process was used to prepare the following glass composition 52S4: (wt%) 52%  $\text{SiO}_2$ –30%  $\text{CaO}$ –14%  $\text{Na}_2\text{O}$ –4%  $\text{P}_2\text{O}_5$ . The glass synthesis was described in detail previously [28]. The glass was prepared in a hermetically cylindrical Teflon container from high-purity raw materials as tetraethyl orthosilicate TEOS:  $\text{Si}(\text{OC}_2\text{H}_5)_4$  (> 98%, Fluka), triethylphosphate TEP:  $\text{OP}(\text{C}_2\text{H}_5)_3$  (> 99.8%, Sigma-Aldrich), calcium carbonate  $\text{CaCO}_3$  (> 98.5%, Merck), and sodium carbonate  $\text{Na}_2\text{CO}_3$  (> 99.5%, Merck). Accurately weighed amounts of these reactants were added, one by one each hour under magnetic stirring, to a 2 M aqueous acetic

acidic solution. The resultant sol was kept for hydrolysis and polycondensation at room temperature for 6 days. After that, it was kept at 70 °C for 3 days and dried at 150 °C for 52 h.

In this study, 52S4 glass is studied in two different microstructural forms (amorphous and partially crystalline). The obtained dried gel was thermally treated at 600 and 650 °C (noted SGDG600 and SGDG650) during 3 h under vacuum with a heating rate of 0.5 °C  $\text{min}^{-1}$ . Let us remember that the domain of thermal stabilization of the dried gel is between the transition temperature  $T_G$  ( $T_G = 596$  °C) and the crystallization temperature  $T_C$  ( $T_C = 631$  °C) as determined by thermogravimetric associated with differential scanning calorimetry (TG/DSC) analyses [28].

### In vitro assays

To evaluate the kinetic reactivity of the prepared glasses, SBF (SBF-K9 type) was used as soaking solution which has the ion concentrations similar to those in human blood plasma. According to Kokubo's protocol [30], the SBF was prepared by dissolving reagent-grade  $\text{CaCl}_2$ ,  $\text{NaCl}$ ,  $\text{KCl}$ ,  $\text{MgCl}_2 \cdot 6\text{H}_2\text{O}$ ,  $\text{K}_2\text{HPO}_4 \cdot 3\text{H}_2\text{O}$ , and  $\text{NaHCO}_3$  in distilled water. It was buffered at pH 7.4 with (hydroxymethyl)-aminomethane [ $(\text{CH}_2\text{OH})_3\text{CNH}_2$ ] and hydrochloric acid (HCl). The glasses were soaked in SBF in the form of disks. 0.5 g of the dried gel in powder, with particle sizes ranged from 40 to 63  $\mu\text{m}$ , were compacted at 675 MPa under cold uniaxial pressing. After that, the compacted dried gel disks were heat treated under the conditions mentioned before. The ratio between the geometric areas of disks and the volumes of SBF was adjusted to 0.075  $\text{cm}^{-1}$ . The glasses were kept in SBF at 37 °C for time periods ranging from 2 h to 30 days (SBF immersion tests were carried out in triplicate). After soaking, the disks were emerged from SBF, washed with ethanol, and dried in air.

### Material characterization

Different techniques and apparatus were used to study the physical and chemical properties of prepared glasses before and after soaking in SBF. The specific surface area and porosity measurements were performed using multi-point BET, ASAP 2010 Micromeritics. In addition, the phase compositions were identified using X-ray diffraction (XRD) data collected in a Bruker, D8 ADVANCE with a  $\text{CuK}\alpha$  radiation ( $\lambda = 0.154$  nm, filter, Ni, voltage = 30 kV and current = 20 mA, step = 0.05°, scan step time = 10 s). To improve the structural analysis, Fourier-transformed infrared spectroscopy (FTIR) (BRUKER EQUINOX 55) was used. One milligram of material scraped from the glass surface was mixed with dried KBr to perform the FTIR studies. The microstructure of glass surfaces was observed using a scanning electron microscope (SEM) (Hitachi, JSM-6301 F) working at a 7 kV as an accelerating voltage. Before observation and EDS analyses

(Oxford Link INCA), the surfaces were gold-coated (Au 20 wt% Pd) in order to allow surface conduction. For the *in vitro* tests in SBF, inductively coupled plasma-optical emission spectroscopy (ICP-OES) (SPECTRO Ciros Vision) technique was used to evaluate the variations of silicon, calcium, and phosphorous concentrations versus soaking time in SBF.

## Results

### Characteristics of 52S4SGDG before soaking in SBF

#### Specific surface area and pore volume

The BET-specific surface area and pore volume of SGDG decreased when temperature increased from 600 to 650 °C. Their values are in order: 18.26 m<sup>2</sup> g<sup>-1</sup> and 0.058 cm<sup>3</sup> g<sup>-1</sup> (for SGDG600) and 6.00 m<sup>2</sup> g<sup>-1</sup> and 0.013 cm<sup>3</sup> g<sup>-1</sup> (for SGDG650), respectively. Also, the median pore diameter decreased from 127 Å (for SGDG600) to 88.34 Å (for SGDG650).

#### X-ray diffraction

Figure 1 shows the XRD data for SGDG600 and SGDG650. The XRD of SGDG600 showed that the final product is amorphous. However, the data reveal that the glass exhibited a very low crystallization of hydroxyapatite (HA) before any immersion in SBF, as for the glass treated at 550 °C [28]. In addition, two diffusion halos are observed in the range 27–34° and 15–23° (2θ). Analogous maxima were obtained by Martinez et al. in their study of binary glasses SiO<sub>2</sub>-CaO. They attributed the diffraction maximum between 28 and 34° 2θ to the incipient presence of different crystalline phases of calcium silicates, whereas the maximum at 22.5° 2θ to a formation of SiO<sub>2</sub> content in the glass [31]. Otherwise, DRX of SGDG650 confirmed the Na<sub>2</sub>Ca<sub>2</sub>Si<sub>3</sub>O<sub>9</sub> crystallization (ICDD powder diffraction: file no. 22.1455), in a glassy matrix.

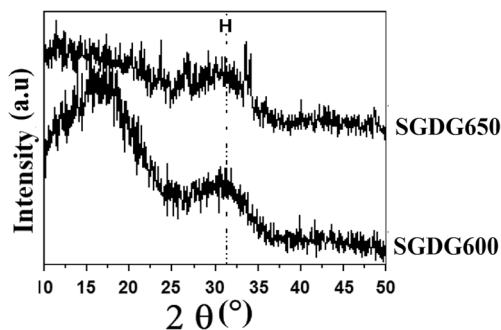


Fig. 1 X-ray diffraction patterns of SGDG heated at 600 and 650 °C. H: HA

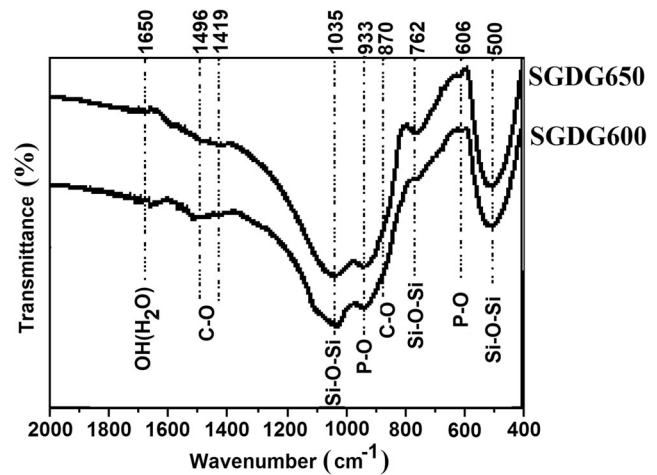


Fig. 2 FTIR spectra of SGDG heated at 600 and 650 °C

#### Infrared studies

Figure 2 shows the FTIR spectra of glasses treated at 600 and 650 °C. As discussed in previous work [28], the observed bands at 500, 762, and 1035 cm<sup>-1</sup> are assigned to silicate network vibrations Si-O-Si. The band observed at 606 cm<sup>-1</sup> is related to P-O bending in crystalline HA [32, 33]. This band was reinforced for glass treated at 650 °C, which confirms the crystallization of HA during heat treatment. In the other hand, the band located at 500 cm<sup>-1</sup> becomes more intense when the temperature increases. This band may be attributed to the crystal phase Na<sub>2</sub>Ca<sub>2</sub>Si<sub>3</sub>O<sub>9</sub> [24, 34]. The bands at 933 and 762 cm<sup>-1</sup>, related to Si-O-Si stretching of non-bridging oxygen atoms [33], are better defined in all spectra. The weak bands at 870, 1419, and 1496 cm<sup>-1</sup> are related to the presence of CO<sub>3</sub><sup>2-</sup> groups [35].

#### In vitro assay results

In order to evaluate the formation kinetics of bone-like apatite at surface of soaked glass in SBF, the pH and variations in Si, Ca, and P concentrations in SBF were quantified versus soaking time. The study was also accomplished by analyzing the formed apatite layer at the glasses surface by XRD, FTIR, and SEM-EDS techniques.

#### ICP results and pH measurements

Figure 3 presents ICP results and pH measurements. The Ca concentration evolution followed a similar tendency for the two materials (Fig. 3a). For both materials, it decreased slowly at the first soaking hours. After that, for SGDG600, this concentration increased slowly until 1 day where it increased dramatically and reached a maximum value. The maximum calcium release from glass surface is achieved after 7 days. After that, a continuous decrease in Ca concentration was observed up to 30 days. For SGDG650, the maximum value

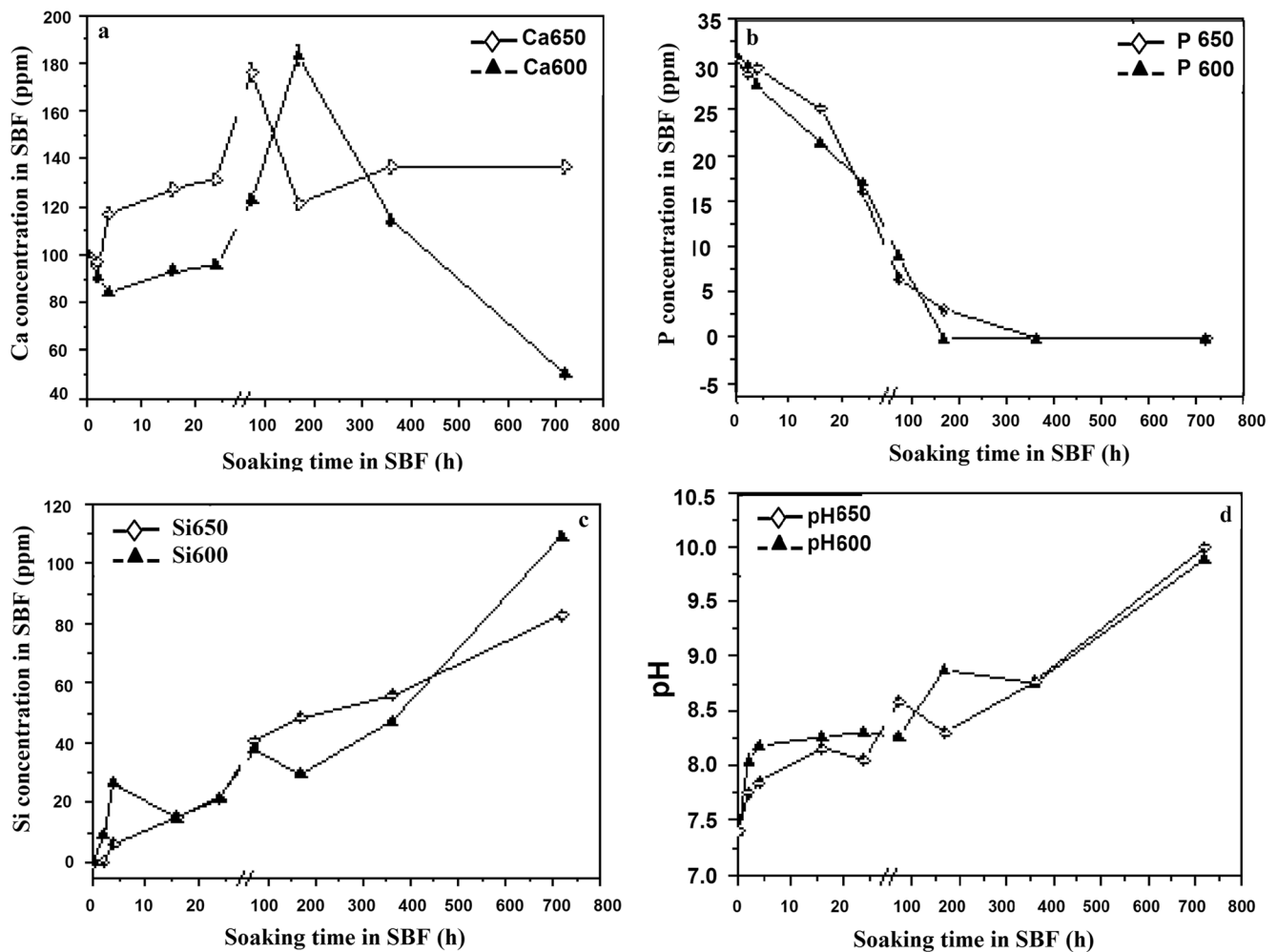


**Fig. 3** Evolutions of Ca (a), P (b), and Si (c) concentrations in SBF, and evolution of SBF pH (d) versus soaking time of SGDGD heated at 600 and 650 °C

for the Ca concentration in SBF was reached after 3 days, then decreased strongly and remained constant in the interval time 7–30 days.

During the experiment, P concentrations in SBF decreased continually (Fig. 3b) for the both materials. This indicates that the amount of P released from glass or glass-ceramic surfaces did not compensate its consumption due to the apatite formation. It can be observed that P concentrations were nil in SBF where SGDGD600 was soaked after 7 days and after 15 days for SGDGD650. All P ions were consumed from SBF.

The increase in Ca concentration in SBF is a result of Ca ions leaching from SGDGD surface to SBF. However, the decrease in the Ca and P concentrations in SBF is attributed to the rapid growth of the apatite at the glass surface that overcame the release rate of Ca and P ions to SBF [31].

As SBF is initially silicon-free, the presence of Si in SBF is consistent with a release of this element from the glass surface to the soaking solution. The Si concentration in SBF increased with soaking time for both materials (Fig. 3c). The Si concentration increased strongly in the first hours for SGDGD600 and

SGDGD650. However, there was a fluctuation in Si concentration during soaking time from 16 h to 15 days for SGDGD600. For SGDGD650, the increase in Si concentration was continuous.

The pH evolution is relevant to the dissolution process of glasses soaked in physiological solutions. The increase in pH of SBF is the result of ion exchanges between the protons  $H^+$  in SBF and the glass-modifying cations. The pH value of SBF increased strongly after 2 h soaking time for both glasses (Fig. 3d). For SGDGD600, the pH was stable around 8.3 between 4 h and 1 day. The increase in pH values was not continuous: a fluctuation occurred in the interval 3–15 days. Between 3 and 7 days, the increase in pH value was followed by a slight decrease between 7 and 15 days. A more noticeable increase in pH value occurred after 30 days. It achieved 9.9 units. For SGDGD650, pH evolution follows the same trend than that of SGDGD600. However, the fluctuation in pH values occurred in the 1–7 days interval. After that, an important increase occurred in pH value which achieved 10 units after 30 days. In general, the pH values for SGDGD650 were lower than that of SGDGD600.

### Structural modifications after soaking in SBF

**XRD results** According to XRD data for SGD600 surface, after soaking in SBF (Fig. 4), crystalline HA peaks appeared only after 15 days (natural HA, prepared from calcined bovine bone, was used as a reference [7]). Before 15 days, it is difficult to distinguish this phase. Noted that after 7 days, the XRD data revealed the formation of calcite, justified by the apparition of its most intense peak at 29.4° (2θ) (ICDD powder diffraction, file no. 86.2334). The intensity of this peak increased with time and it became a major visible phase on XRD diagram after 30 days. As a consequence, the intensity of crystallized HA peaks decreased between 15 and 30 days.

For SGD650, the crystalline HA peaks appeared on the XRD pattern after 2 h. The peaks intensity of HA increased after 4 h. Additionally, XRD highlighted the presence of Na<sub>2</sub>Ca<sub>2</sub>Si<sub>3</sub>O<sub>9</sub> phase at the same time. This latter phase became the dominant crystallized phase after 16 h, as the peaks intensity of HA became lower. Between 4 h and 1 day, XRD also revealed the presence of an amorphous phase at the glass-ceramic surface. A broad halo appeared around 20 °C which can be attributed to silica gel [36]. After that, the peaks intensity of HA increased and those of Na<sub>2</sub>Ca<sub>2</sub>Si<sub>3</sub>O<sub>9</sub> decreased up to 7 days when the peaks intensity of the two phases were similar. After 15 days, Na<sub>2</sub>Ca<sub>2</sub>Si<sub>3</sub>O<sub>9</sub> appeared again as the mainly formed phase. After 30 days, the calcite peak was present. Consequently, it can be observed that the peaks intensities of previous existent phases HA and Na<sub>2</sub>Ca<sub>2</sub>Si<sub>3</sub>O<sub>9</sub> decreased strongly.

**FTIR results** In SGD600 spectra (Fig. 5a), between 2 and 4 h, the characteristic peaks of amorphous HA appeared at 464 cm<sup>-1</sup> and a broadening band situated around 1056 cm<sup>-1</sup> [33]. The presence of crystallized HA was confirmed after 16 h by the apparition of a weak, new peak at 560 cm<sup>-1</sup> and reinforcement of band situated at 605 cm<sup>-1</sup>. These bands are distinguishable until 15 days. Additionally, the characteristic bands of C-O vibrations, mainly attributable to calcite, appeared after 7 days and are clearly visible after 15 days. Also, these bands can be attributed to C-O in carbonated

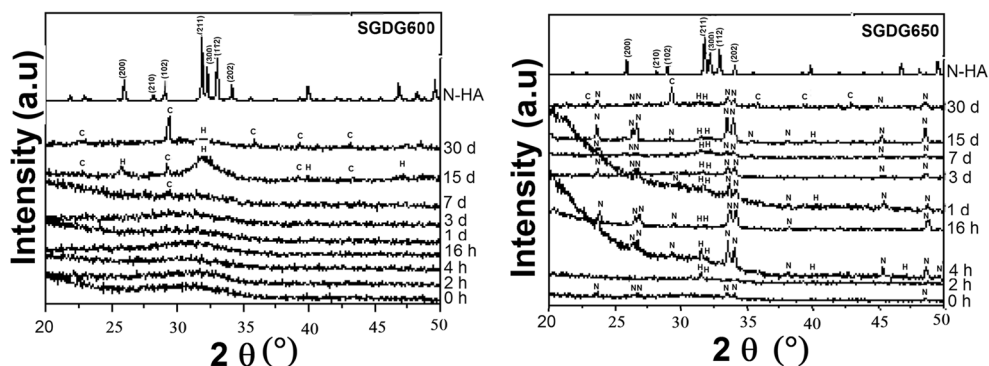
HA. As indicated by XRD, after 30 days, the calcite was present simultaneously with crystallized HA. In IR spectra, the characteristic bands of glass network progressively disappeared with time which led to conclude that carbonated HA layer is dense.

A new, weak band at 823 cm<sup>-1</sup>, characteristic of Si-O symmetric stretching vibrations [33, 37], appeared after 1 day. This band was also present until 15 days. This result confirms the formation of a Si-rich layer at the glass surface.

For SGD650 (Fig. 5b), no difference appeared between spectra before soaking and after 2 h in SBF. After 4 h, the characteristic bands of P-O appeared at 454, 533 cm<sup>-1</sup> and a weak band at about 610 cm<sup>-1</sup>. These bands confirmed the formation of crystallized HA. These bands were reinforced until 3 days. After 7 days, the intensity of the band situated at 533 cm<sup>-1</sup> decreased and another band, characteristic of P-O vibration in crystallized HA, appeared at 562 cm<sup>-1</sup>. No change occurred after 15 days. After 30 days, the band situated at 533 cm<sup>-1</sup> merged in the band situated at 562 cm<sup>-1</sup>. In addition, the intensity of the band situated at 610 cm<sup>-1</sup> decreased. It can be observed that the intensity of the band at 933 cm<sup>-1</sup>, related to Si-O-Si vibration, decreased with soaking time. Also, the band around 1040 cm<sup>-1</sup> becomes sharp and two other characteristic bands of P-O in HA appeared at 1045 and 1085 cm<sup>-1</sup>. The characteristic bands of C-O situated at 870, 1420, and 1496 cm<sup>-1</sup> were clearly visible after 3 days which led to conclude that the formed apatite is carbonated HA. These bands were also well noticeable after 30 days. According to XRD results, these bands are attributable to CaCO<sub>3</sub> phase and carbonated HA. A weak band appeared at 800 cm<sup>-1</sup> [33, 37], which is a characteristic band of Si-O symmetric stretching vibrations, after 4 h and 1 day. This band reappeared strongly after 7 days. Hence, the FTIR results are in a good agreement with the XRD results.

**SEM-EDS results** SEM images and EDS analyses (Fig. 6) depicted the morphological modifications and composition evolutions of SGD600 surface with soaking time. After 2 h, a new layer, formed by spherical particles, dispersed at the glass surface. The EDS analysis, with the significant

**Fig. 4** XRD patterns of SGD600 and SGD650 surfaces before and after soaking in SBF solution at different testing times. H, HA; C, CaCO<sub>3</sub>; N, Na<sub>2</sub>Ca<sub>2</sub>Si<sub>3</sub>O<sub>9</sub>



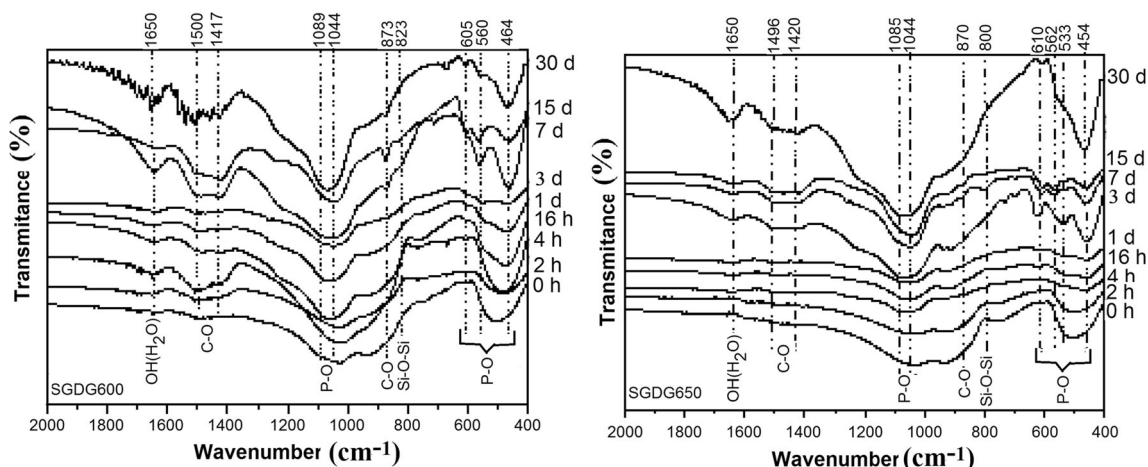


Fig. 5 FTIR spectra of SGD600 and SGD650 before and after soaking in SBF

increase in phosphorous concentration, confirmed the formation of an apatite layer at the glass surface after 2 h in SBF as suggested by FTIR and ICP results. This layer becomes denser with time. However, after 30 days, the Ca and P concentrations decreased. According to the ICP result, the P concentration was nil between 7 and 30 days. So, there were no P ions to lead to continuous apatite formation. In addition, SBF is saturated by carbonate ions which led to calcite formation up to crystallized carbonated HA (the characteristic rhombohedral particles of  $\text{CaCO}_3$  as calcite were not observed at the glass surface, giving evidence of the presence of this phase as localized precipitate and not as surface-controlled phase).

The Si concentration decreased at the glass surface after 15 days. This result is consistent with the formation of a dense apatite layer at the glass surface. However, the Si concentration increased after 30 days. This result may be related to the presence of Si in the apatite layer due to the continuous Si release between 7 and 30 days revealed by ICP analyses or to a new visibility of the silica gel formed at 7 days (as evidenced

by IR analysis) due to the impossibility of the apatite layer formation to progress without phosphorous ions in SBF.

The morphological modifications of SGD650 surface with soaking time were depicted by SEM images and EDS analyses (Fig. 7). After 2 h, some spherical particles dispersed on a uniform gel formed at the glass surface. The EDS analysis showed that there was a slight increase in both Si and P concentrations at the glass surface. This layer is attributed to silica gel and the spherical particles to apatite layer, as it was confirmed by XRD and ICP results. After 4 h, the SEM images showed that there were two phases one up to another with different morphologies. The EDS analyses showed a significant increase in P concentration at the glass surface. This result, associated to the ICP analyses ones, is consistent with the formation of the apatite layer, the glass surface up to the silica gel layer. After 1 day, this phase becomes uniform and compact as confirmed by EDS surface analyses. After 3 days, it is very difficult to distinguish the grain boundaries. A formed gel has covered the totality of the last layer. The IR

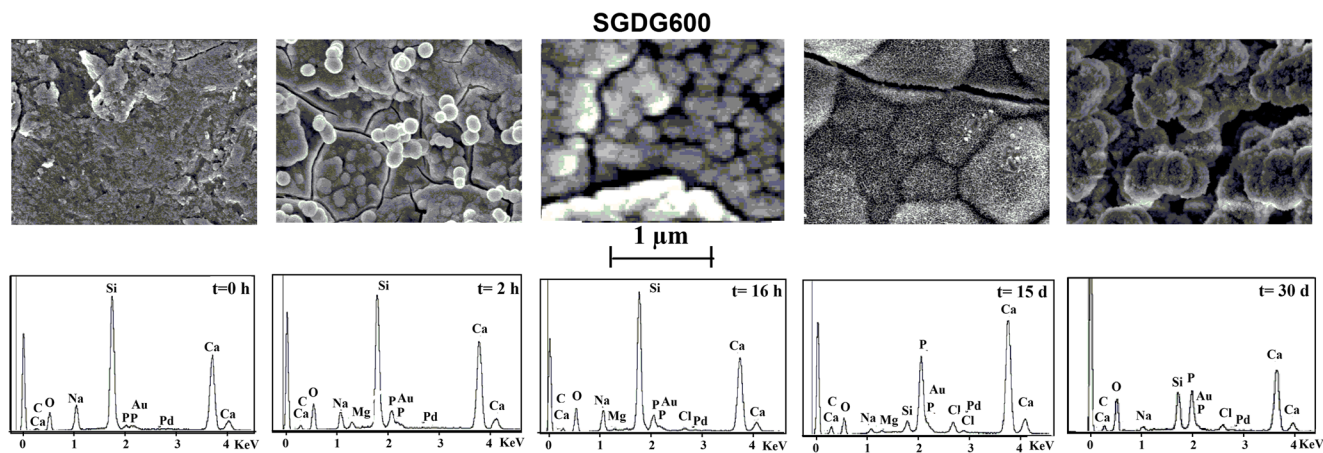


Fig. 6 SEM micrographs and EDS spectra of SGD600 surfaces before and after soaking in SBF

## SGDG650

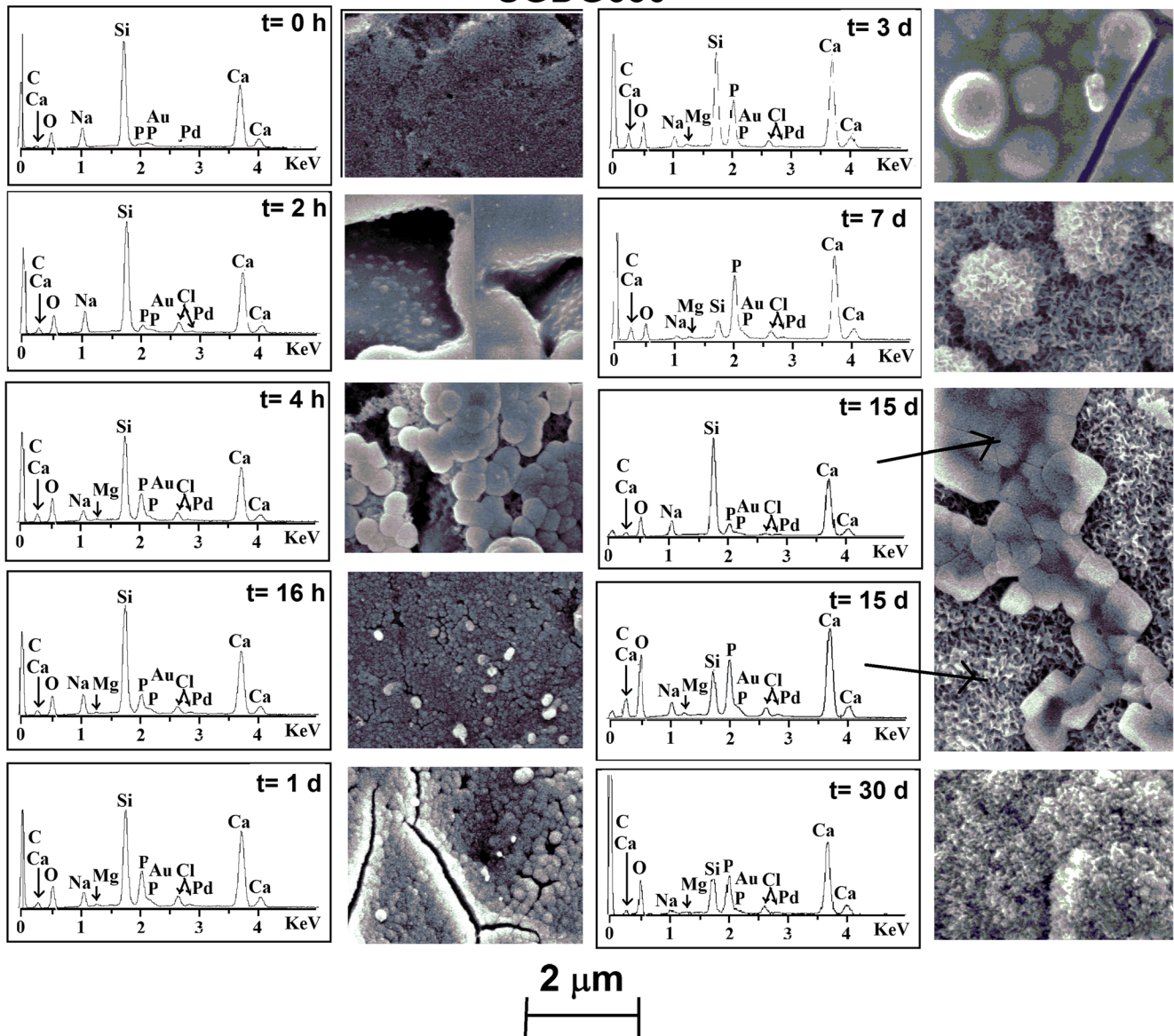


Fig. 7 SEM micrographs and EDS spectra of SGDG650 surfaces before and after soaking in SBF

analysis showed the formation of silica gel justified by appearance of Si-O-Si band at  $800\text{ cm}^{-1}$ . After 7 days, a very dense layer was formed. The entire glass surface was covered with compacted needle-like crystallites, very rich in Ca and P elements, consistent with aggregates of carbonated HA. In addition, the ICP results showed that Ca and P ion concentrations decreased mainly in SBF after 7 days. After 15 days, another phase was formed up to the carbonated HA layer. The EDS analyses showed that one phase was rich in Ca and P ions and poor in Si and Na. The other phase was rich in Si, Na, and Ca and poor in P. According to the XRD diagram, the two phases are HA and  $\text{Na}_2\text{Ca}_2\text{Si}_3\text{O}_9$ . Finally, after 30 days, a new layer was formed at the glass surface. This layer of crystallized HA had a different morphology than that at 15 days.

## Discussion

The heat treatment at  $650\text{ }^\circ\text{C}$ , above the temperature of crystallization outset [28], induced the crystallization of  $\text{Na}_2\text{Ca}_2\text{Si}_3\text{O}_9$  in a mainly amorphous matrix. Compared with the two other materials, SGDG550 [29] and SGDG600, SGDG650 is a glass ceramic.

Results concerning the material bioactivity study, evaluated by soaking material in SBF, indicate that 52S4SGDG glass exhibited special reactivity features directly related to the temperature of heat treatment.

The bioactivity characteristic is associated to the occurrence of successive steps. As described by Hench for bioactive glasses [38] and Kokubo [39] for bioactive

materials containing CaO-SiO<sub>2</sub>, a hydrated silica layer is formed at the surface prior to the deposition of HA. After rapid exchange of glass-modifier cations (Na<sup>+</sup> and/or Ca<sup>2+</sup>) with H<sup>+</sup> in solution, the soluble silica is loosened as Si(OH)<sub>4</sub> by breaking of Si-O-Si bridges and subsequent silanol Si-OH groups are formed at the material surface. After that, silanol groups condense and their polymerization forms a SiO<sub>2</sub>-rich surface layer. Silica gel thickness increases with glass surface leaching [40]. Up to this layer, CaO-P<sub>2</sub>O<sub>5</sub>-rich layer forms and further crystallized as carbonated HA layer [38, 41–43]. The nuclei thus formed later grow at the expense of the ions in the solution that was saturated with respect to apatite. Kim et al. [44] reported that glasses with < 50 mol% SiO<sub>2</sub> form a Ca-P-rich layer and a Si layer simultaneously, while glasses with > 50 mol% SiO<sub>2</sub> form a Ca-P layer on the top of a Si-rich layer. These differences are related to the glass structure in relation with composition.

Dissolution rates and SiO<sub>2</sub>-rich layer formation are mainly associated to the evolution of silicon concentration and pH of SBF. Also, the formation of carbonated HA layer is associated to the evolution of calcium and phosphorous concentrations in SBF. Obtained results indicate that the three different materials, SGD550, SGD600, and SGD650, presented different features.

By comparing to the previous ICP results [29], SGD600 has similar behavior than SGD550 up to 4 h soaking: an important release of silicon and an increase of pH above 8. During this time, calcium and phosphorous concentrations decrease in SBF for the two glasses. As confirmed by ICP, XRD, IR, and EDS results, the formation of carbonated HA layer occurred simultaneously to the glasses' dissolution. These results are in accordance with those of Kim et al. [44] who reported that glasses with 50 mol% SiO<sub>2</sub> form a Ca-P-rich layer and a Si layer simultaneously. Our glass contains 52.3% SiO<sub>2</sub> close to 50% mol.

In our previous work for SGD550 [29], Si concentration in SBF increased up to 3 days before a decrease which was consistent with the formation of the SiO<sub>2</sub> layer. The successive silica layers were formed during soaking time simultaneously with carbonated HA layers. XRD and FTIR analyses showed that no crystallized apatite phase was formed at the SGD550 surface even after 30 days. But, after 2 h, the calcite was formed at the glass surface. This phase was previously observed for a glass with a molar composition 60% SiO<sub>2</sub>-35% CaO-5% P<sub>2</sub>O<sub>5</sub> [45]. The presence of this phase is not related to the glass composition but due to the high concentration of HCO<sub>3</sub><sup>-</sup> in SBF that induced, in the presence of high calcium concentrations near the glass surface, the calcite CaCO<sub>3</sub> precipitation instead of the surface-controlled crystallization of carbonated HA.

For SGD600, after 4 h, a decrease in Si concentration in SBF was observed. This is consistent with the formation of the SiO<sub>2</sub> layer at the material surface after 1 day. This silica layer was already detected until 30 days. Between 4 h and 7 days, the glass dissolution process is the dominant feature compared to the carbonated HA precipitation process. After 7 days, the HA precipitation predominated the dissolution process as indicated by the decrease of Ca and P concentrations in SBF. IR analysis highlighted the presence of a carbonated apatitic phase between 1 and 7 days. This phase was well crystallized after 15 days as confirmed by the XRD and IR results.

The secondary precipitation of calcite CaCO<sub>3</sub> is observed after 30 days. This phenomenon is amplified by the total consumption of SBF phosphorous ions after 7 days. As consequence, there were no P ions to allow the continuous apatite formation.

For SGD650 during the periods 0–4 h, the silicon release is slower than the two other materials and the pH stays under 8. The pH value stayed under 8 and slowed down the Si dissolution [46] which inhibited the formation of silanol groups Si-OH at the glass surface and consequently their release as Si(OH)<sub>4</sub>. These results may be related to a lower reactivity of glass ceramic due to the significant reduction of specific surface area and pore volume for SGD650 comparatively to the other materials associated to a difference in the reaction mechanism related to the presence of the crystallized phase associated to the glass matrix, which induced an inhomogeneity in the reactivity of the material surface.

During the two first hours, the glass ceramic dissolved weakly and a calcium and phosphorous ion uptake by the material surface occurred. The silica gel layer was detected only by SEM analysis; the thickness of this layer was weak and consequently not detectable by IR analysis. Up to this silica layer, the carbonated HA spherical particles were formed as justified by the XRD, IR, and MEB-EDS results. However, from 2 h to 7 days, a more complex process setup: an important release of calcium from the material occurred. This release was not associated to a proportional release of silicon in SBF. The material dissolution is associated to the simultaneous formation of a new amorphous phase and the reformation of Na<sub>2</sub>Ca<sub>2</sub>Si<sub>3</sub>O<sub>9</sub> at the material surface as shown in XRD diagrams. In parallel, between 4 h and 3 days, the Ca and P concentrations at the glass surface increased as demonstrated by EDS analysis which confirms the formation of CHA layer, its densification, and grain size enlargement with time. The IR and XRD analysis confirmed this result, the intensity of P-O bands increased with time and the intensity of characteristic XRD peaks of Na<sub>2</sub>Ca<sub>2</sub>Si<sub>3</sub>O<sub>9</sub> decreased with the continuous formation of carbonated HA layer. This particular behavior may be related to the initial presence of Na<sub>2</sub>Ca<sub>2</sub>Si<sub>3</sub>O<sub>9</sub> which had a different dissolution rate from the glass matrix. The consistency between the obtained results shows that the dissolution of



$\text{Na}_2\text{Ca}_2\text{Si}_3\text{O}_9$  was followed by a reprecipitation of this phase at the glass surface, associated to a rapid formation of the calcium-free amorphous silicon-rich phase and a consecutive formation of the carbonated HA. After 7 days, the Ca and P concentrations in SBF decrease as those at the glass surface achieved their maximum values which are consistent with the densification of CHA layer and its formation as compacted needle-like crystallites' aggregates. After 15 days, all P ions in SBF were consumed, and then, after 15 days, there were no P ions available to form HA. Calcium ion concentration increased slightly and stabilized between 7 and 30 days as silicon concentration increased continuously during soaking time. These results indicate that the material dissolution went out. The CHA formation was stopped by lack of phosphorous in SBF and up to 15 days, the reprecipitation of  $\text{Na}_2\text{Ca}_2\text{Si}_3\text{O}_9$  is favored. After 30 days, the calcite ( $\text{CaCO}_3$ ) was formed, up to  $\text{Na}_2\text{Ca}_2\text{Si}_3\text{O}_9$ , by the combination of calcium ions from glass and  $\text{HCO}_3^-$  from SBF [45].

As described in previous work [29], higher specific surface area and pore volume in sol-gel-derived glass (SGDG550) than in melting-derived glass (MDG) favored the formation of the bone-like apatite layer after 2 h soaking in SBF. For MDG, the bone-like apatite layer was formed after 1 day soaking in SBF. In addition, the dissolution process was only observed in MDG; the Ca and P have been released from MDG surface for 7 days. After this time, the Ca and P concentrations decreased in SBF. However, for SGDG550, Ca and P concentrations decreased in SBF at the beginning of soaking which confirms the domination of precipitation process during soaking in SBF. The specific surface area and pore volume are the key factors of glass reactivity. So, when the values of these parameters are altered, the process of dissolution-precipitation will be also affected. In this work, the temperature treatment has a marked effect on the value of the specific surface area and pore volume: when the heat temperature increases, the surface area and the pore volume decrease. Consequently, the kinetic of ionic exchanges decreases, between material and surrounding medium. According to obtained results, when the temperature increases from 600 to 650 °C, the specific surface area and pore volume porosity of the glass decrease and the crystallized phase  $\text{Na}_2\text{Ca}_2\text{Si}_3\text{O}_9$  is formed. At the same time, the corresponding time of dissolution onset decreases. So, the crystallization of glass and decrease of the value of surface area affected the kinetic of the dissolution process. These results are in accordance with previous studies. Peitl et al. showed that glass crystallization decreased the kinetics of the CHA layer development [24]. Other researchers demonstrated that glass ceramics may be less soluble in body fluid and that the mineral

formation rate and bone integration at the tissue-material interface may be affected [22–24]. The crystallization of some glassy systems significantly decreases their bioactivity in comparison with the same amorphous glassy systems [19–21].

Note that the CHA was formed after 2 h at glass surface for all treatment temperatures. However, the corresponding time to carbonated HA crystallization decreases with heat treatment. Moreover, the corresponding time for apparition of characteristic bands of silica gel increases with treatment temperature. It was suggested, for SGDG550, that the continuous formation of silica gel at the glass surface during the soaking time inhibited the HA crystallization. For SGDG600 and SGDG650, the thickness of silica layers was thinner and their formation were limited comparatively to SGDG550, which allowed the HA crystallization.

In this work, a special behavior was observed for SGDG650;  $\text{Na}_2\text{Ca}_2\text{Si}_3\text{O}_9$  phase, initially present in the material, was reprecipitated at the material surface during soaking time. It can be suggested that the dissolution of this phase occurred and the diffusion of ions promoted the formation of this phase at the glass surface.

So, the heat treatment and the formation of the crystallized phases such as  $\text{Na}_2\text{Ca}_2\text{Si}_3\text{O}_9$  maintained the high bioactivity of 52S4 as other particular compositions of the  $\text{SiO}_2\text{--CaO--Na}_2\text{O--P}_2\text{O}_5$  system in other works [23, 24, 27, 47–50]. Moreover, the heat treatment at 600 and 650 °C allowed the HA crystallization not observed for the glass treated at 550 °C even after 30 days for which HA phase remained amorphous.

## Conclusion

The obtained results lead to conclude that the bioactivity of 52S4SGDG glass was not affected by the heat treatment modification. For all temperatures, carbonated HA was formed at the material surface after soaking in SBF. For SGDG550, the carbonated HA remained amorphous even after 30 days and it was formed up to the silica layer which reformed at any time. For SGDG600, carbonated HA began to crystallize after 16 h and became well crystallized after 15 days. However, the heat treatment at this temperature did not prevent the reformation of a silicon oxide layer up to the carbonated HA one. The silica layer was detected later than the carbonated HA formation, accordingly to IR results. Otherwise, for SGDG650, the crystallized carbonated HA was observed after 2 h. In addition, the crystallized phase  $\text{Na}_2\text{Ca}_2\text{Si}_3\text{O}_9$  in the initial material before soaking was reprecipitated at the glass surface after 15 days.

This study highlighted the original behavior of this new composition and the possible adjustment of reactivity by

modifying the heat treatment temperature, without changing the material bioactive features.

**Acknowledgements** Many thanks to Bernard Lefevre (Equipe Verres et Céramiques, UMR 6226 Rennes), F. Gouttefangeas (CMEBA Centre of UMR-CNRS 6226- Rennes), and D. Laillé (INSA- Rennes) for their fruitful collaborations.

**Funding information** The authors would like to thank the authorities responsible for the financial support of this work (M'sila University and Algerian minister of superior education and research).

## References

- Hench, L.L., Splinter, R.J., Allen, W.C., Greenlee, T.K.: Bonding mechanism at the interface of ceramics prosthetic materials. *J Biomed Mater Res Symp.* **2**, 117–141 (1971)
- Hench, L.L.: The story of bioglass. *J Mater Sci Mater Med.* **17**, 967–978 (2006)
- Kokubo, T.: Bioactive glass ceramics: properties and applications. *Biomaterials.* **12**, 155–163 (1991)
- LeGeros, R.Z.: Properties of osteoconductive biomaterials: calcium phosphates. *Clin Orthop Relat Res.* **395**, 81–98 (2002)
- Mezahi, F.Z., Harabi, A., Achour, S.: Effect of stabilised ZrO<sub>2</sub> on sintering of hydroxyapatite. *Key Eng Mater.* **264**, 2031–268, 2034 (2004)
- Mezahi, F.Z., Harabi, A., Zouai, S., Achour, S., Bernache-Assollant, D.: Effect of stabilised ZrO<sub>2</sub>, Al<sub>2</sub>O<sub>3</sub> and TiO<sub>2</sub> on sintering of hydroxyapatite. *Mater Sci Forum.* **492**, 241–493, 248 (2005)
- Mezahi, F.Z., Oudadesse, H., Harabi, A., Lucas-Girot, A., Le Gal, Y., Chaair, H., Cathelineau, G.: Dissolution kinetic and structural behaviour of natural hydroxyapatite vs. thermal treatment : comparison to synthetic hydroxyapatite. *J Thermal Anal Calor.* **95**(1), 21–29 (2009)
- Harabi, A., Belamri, D., Karboua, N., Mezahi, F.Z.: Sintering of bioceramics using a modified domestic microwave oven. *J Therm Anal Calorim.* **104**, 283–289 (2011)
- Mezahi, F.Z., Oudadesse, H., Harabi, A., Lucas-Girot, A.: Effect of ZrO<sub>2</sub>, TiO<sub>2</sub>, and Al<sub>2</sub>O<sub>3</sub> additions on process and kinetics of bonelike apatite formation on sintered natural hydroxyapatite surfaces. *Int J Appl Ceram Technol.* **9**, 529–540 (2012)
- Harabi, A., Harabi, E., Chehalatt, S., Zouai, S., Karboua, N.E., Foughali, L.: Effect of B<sub>2</sub>O<sub>3</sub> on mechanical properties of porous natural hydroxyapatite derived from cortical bovine bones sintered at 1050°C. *Des Wat Treat.* **57**(12), 5303–5309 (2016)
- Harabi, E., Harabi, A., Mezahi, F.Z., Zouai, S., Karboua, N.E., Chehalatt, S.: Effect of P<sub>2</sub>O<sub>5</sub> on mechanical properties of porous natural hydroxyapatite derived from cortical bovine bones sintered at 1050°C. *Des Wat Treat.* **57**(12), 5297–5302 (2016)
- Harabi, E., Harabi, A., Foughali, L., Chehlatt, S., Zouai, S., Mezahi, F.Z.: Grain growth in sintered natural hydroxyapatite. *Acta Phy Polonica A.* **127**(4), 1161–1163 (2015)
- Harabi, A., Harabi, E.: A modified milling system, using a bimodal distribution of highly resistant ceramics. Part I: a natural hydroxyapatite study. *Mater Sci Eng (C).* **51**, 206–215 (2015)
- Harabi, A., Chehlatt, S.: Preparation process of a highly resistant wollastonite bioceramics using local raw materials. *J Therm Anal Calorim.* **111**, 203–211 (2013)
- Chehlatt, S., Harabi, A., Harabi, E., Zouai, S., Oudadesse, H., Barama, S.E.: Biological properties study of bioactive wollastonite containing 5 wt% B<sub>2</sub>O<sub>3</sub> prepared from local raw materials. *Des Wat Treat.* **57**(12), 5292–5296 (2016)
- Chehlatt, S., Harabi, A., Oudadesse, H., Harabi, E.: In vitro bioactivity study of pure wollastonite prepared from local raw materials. *Acta Phy Polonica A.* **127**(4), 925–927 (2015)
- Zouai, S., Mezahi, F., Achour, S., Harabi, A.: A process for sintering of diopside prepared from dolomite. *Mater Sci Forum.* **492**, 235–493, 240 (2005)
- Harabi, A., Zouai, S.: A new and economic approach to synthesize and fabricate bioactive diopside ceramics using a modified domestic microwave oven. Part I: study of sintering and bioactivity. *Int J Appl Ceram Technol.* **11**, 31–46 (2014)
- Kokubo T, Bioceramics and their clinical applications. Kokubo T, Eds, Boca Raton, Florida: CRC Press, 2008
- Hench, L.L.: Biomaterials: a forecast for the future. *Biomaterials.* **19**, 1419–1423 (1998)
- De Aza, P.N., De Aza, A.H., Pena, P., De Aza, S.: Bioactive glasses and glass ceramics. *Bol Soc Esp Ceram.* **46**, 45–55 (2007)
- Greenlee Jr., T.K., Beckham, C.A., Crebo, A.R., Malmorg, J.C.: Glass ceramic bone implants. *J Biomed Mater Res.* **6**(3), 235–244 (1972)
- Peitl, O., La Torre, G.P., Hench, L.L.: Effect of crystallization on apatite layer formation on bioactive glass 45S5. *J Biomed Mater Res.* **30**(4), 509–514 (1996)
- Peitl, O., Zanutto, E.D., Hench, L.L.: Highly bioactive P<sub>2</sub>O<sub>5</sub>-Na<sub>2</sub>O-CaO-SiO<sub>2</sub> glass-ceramics. *J Non-Cryst Solids.* **292**(1), 115–126 (2001)
- Li, P., Yang, Q., Zhang, F., Kokubo, T.: The effect of residual glassy phase in a bioactive glass-ceramic on the formation of its surface apatite layer in vitro. *J Mater Sci Mater Med.* **3**, 452–456 (1992)
- Zanutto E.D., Ravagnani C., Peitl O., Panzeri H. Lara E.H.G.: Process and compositions for preparing particulate, bioactive or resorbable biosilicates for use in the treatment of oral ailments, Patent WO/2004/074199, September 02 (2004)
- Siqueira, R.L., Peitl, O., Zanutto, E.D.: Gel-derived SiO<sub>2</sub>-CaO-Na<sub>2</sub>O-P<sub>2</sub>O<sub>5</sub> bioactive powders: synthesis and in vitro bioactivity. *Mater Sci Eng C.* **31**(5), 983–991 (2011)
- Lucas-Girot, A., Mezahi, F.Z., Mami, M., Oudadesse, H., Harabi, A., Le Floch, M.: Sol-gel synthesis of a new composition of bioactive glass in the quaternary system SiO<sub>2</sub>-CaO-Na<sub>2</sub>O-P<sub>2</sub>O<sub>5</sub>: comparison with melting method. *J Non-Cryst Solids.* **57**, 3322–3327 (2013)
- Mezahi, F.Z., Lucas-Girot, A., Oudadesse, H., Harabi, A.: Reactivity kinetics of 52S4 glass in the quaternary system SiO<sub>2</sub>-CaO-Na<sub>2</sub>O-P<sub>2</sub>O<sub>5</sub>: influence of the synthesis process: melting versus sol-gel. *J Non-Cryst Solids.* **361**, 111–118 (2013)
- Kokubo, T., Kushitani, H., Sakka, S., Yamamuro, S.T.: Solutions able to reproduce in vivo surface- structure changes in bioactive glass-ceramic A-W. *J Biomed Mater Res.* **24**, 721–734 (1990)
- Martinez, A., Izquierdo-Barba, I., Vallet-Regi, M.: Bioactivity of CaO-SiO<sub>2</sub> binary glasses system. *Chem Mater.* **12**, 3080–3088 (2000)
- Sepulveda, P., Jones, J.R., Hench, L.L.: In vitro dissolution of melt derived 45S5 and sol-gel derived 58S bioactive glasses. *J Biomed Mater Res.* **61**, 301–311 (2002)
- ElBatal, H.A., Azooz, M.A., Khalil, E.M.A., Soltan Monem, A., Hamdy, Y.M.: Characterization of some bioglass-ceramics. *Mater Chem Phys.* **80**, 599–609 (2003)
- Chang, M.L., Tanaka, J.: FT-IR study for hydroxyapatite/collagen nanocomposite cross-linked by glutaraldehyde. *Biomaterials.* **23**, 4811–4818 (2002)
- Moura, J., Teixeira, L.N., Ravagnani, C., Peitl, O., Zanutto, E.D., Beloti, M.M., Panzeri, H., Rosa, A.L., Oliveira, P.T.: In vitro osteogenesis on a highly bioactive glass-ceramic (Biosilicate®). *J Biomed Mater Res.* **82**, 545–547 (2007)

36. Aina, V., Bertinetti, L., Cerrato, G., Cerruti, M., Lusvardi, G., Malavasi, G., Morterra, C., Tacconi, L., Menabue, L.: On the dissolution/reaction of small-grain Bioglass® 45S5 and F-modified bioactive glasses in artificial saliva (AS). *J Appl Surf Sci.* **257**, 4185–4195 (2011)
37. Vallet-Regi, M., Romero, A.M., Ragel, C.V., Le Geros, R.Z.: XRD, SEM-EDS, and FTIR studies of in vitro growth of an apatite-like layer on sol-gel glasses. *J Biomed Mater Res.* **44**(4), 416–421 (1999)
38. Hench, L.L.: Bioceramics—from concept to clinic. *J Am Ceram Soc.* **74**, 1487–1510 (1991)
39. Kokubo, T.: Novel bioactive materials. *Anales de quimica Int Ed.* **93**, 49–55 (1997)
40. Ebisawa, Y., Kokubo, T., Ohura, K., Yamamuro, T.: Bioactivity of Fe<sub>2</sub>O<sub>3</sub> containing CaOSiO<sub>2</sub> glasses: in vitro evaluation. *J. Mater. Sci: Mater. Med.* **4**, 225–232 (1992)
41. Kokubo T, Yamamuro T, Hench LL, *Handbook of bioactive ceramics. Vol. 1*, Hench LL, Wilson J, Eds. Boca Raton, Florida: CRC Press, 1990: 41–49.
42. Li, P., Ohtsuki, C., Kokubo, T., Nakanishi, K., Soga, N., Nakamura, T., Yamamuro, T.: Process of formation of bone-like apatite layer on silica gel. *J Mater Sci Mater Med.* **4**, 127–113 (1993)
43. Li, P., Ye, X., Kangasniemi, I., de Blicke-Hogervorst, J.M.A., Klein, C.P.A.T., Groot, K.: In vivo calcium phosphate formation induced by sol-gel- prepared silica. *J Mater Res.* **29**, 325–328 (1995)
44. Kim, C.Y., Clark, A.E., Hench, L.L.: Compositional dependence of calcium-phosphate layer formation in fluoride bioglasses. *J Biomed Mater Res.* **26**, 1147–1161 (1992)
45. Mami, M., Lucas-Girot, A., Oudadesse, H., Dorbez-Sridi, R., Mezahi, F.Z., Dietrich, E.: Investigation of the surface reactivity of a sol-gel derived glass in the ternary system SiO<sub>2</sub>–CaO–P<sub>2</sub>O<sub>5</sub>. *App Sur Sc.* **254**, 7386–7393 (2008)
46. Iler RK. *The chemistry of silica: solubility, polymerization, colloid and surface properties and biochemistry.* Wiley J & Sons, Eds. New York: Wiley Interscience, 1979: 453–462
47. Chen, Q.Z., Thompson, I.D., Boccaccini, A.R.: 45S5 Bioglass®-derived glass-ceramic scaffolds for bone tissue engineering. *Biomaterials.* **27**, 2414–2425 (2006)
48. Boccaccini, A.R., Chen, Q., Lefebvre, L., Gremillard, L., Chevalier, J.: Sintering, crystallisation and biodegradation behaviour of Bioglass®-derived glass-ceramics. *Faraday Discuss.* **136**, 27–44 (2007)
49. Huang, R., Pan, J., Boccaccini, A.R., Chen, Q.Z.: A two-scale model for simultaneous sintering and crystallization of glass-ceramic scaffolds for tissue engineering. *Acta Biomater.* **4**, 1095–1103 (2008)
50. Bretcanu, O., Samaille, C., Boccaccini, A.R.: Simple methods to fabricate Bioglass-derived glass-ceramic scaffolds exhibiting porosity gradient. *J Mater Sci.* **43**, 4127–4134 (2008)